Strain Gradients in Poly-SiGe Nanocantilevers: Experimental and Finite Element Modeling Studies

T. B. Asafa

Ladoke Akintola University of Technology, P.M.B. 4000, Ogbomoso, Nigeria, tbasafa@lautech.edu.ng
KACST-Intel Consortium Center of Excellence in Nano-manufacturing Applications, Saudi Arabia

ABSTRACT

One of the fundamental structural requirements for successful performance of Micro/Nano-ElectroMechanical (M/NEM) devices is low strain gradient. Experimental measurement of strain gradient consumes much time, therefore developing a simple method is necessary. In this paper, a comparative study of strain gradients in polycrystalline silicon germanium (poly-SiGe) nanocantilevers measured experimentally and estimated via finite element modeling (FEM) approaches is reported. Arrays of nanocantilevers were fabricated from ~100 nm thick poly-SiGe films via micromachining. Subsequently, strain gradients were calculated from the tip deflections. Then, the cantilevers are modelled using COMSOL multiphysics as superposition of smaller layers, with each later sustaining its corresponding local stress. For the two films (A and B) considered, the experimental average strain gradient differs from that of FEM by ~5% and ~6%, respectively with standard deviations lying between ±0.004 and ±0.009.

Key words: Poly-SiGe, strain gradient, FEM, COMSOL.

1 INTRODUCTION

Polycrystalline silicon germanium (poly-SiGe) films are now being used to fabricate various technological devices including gyroscopes, low frequency comb drives, micromirrors among others [1]. These applications are feasible because of the low thermal budget for poly-SiGe film deposition (<450^{o}C) which has proven useful when monolithically integrating M/NEMS with its driving electronic components in the MEMS-last approach [1, 2].

One of the most important characteristics of M/NEM devices such as nanoswitches, nanoresonators and biosensors is strain gradient. Excessive strain gradient causes a released structure to bend upward or downward which consequently alters the dynamic and reliability characteristics of devices made therefrom. Taking bioresonators for examples, excessive downward bending can lead to stiction and causes a change in the resonance frequency. For applications such as resonators, excessive upward bending is detrimental to the pull-in and pull-out voltages as well as the resonance frequency.

Experimentally, strain gradients can be calculated from the tip deflections of free-standing cantilevers which are fabricated by surface micromachining [2]. However, this method consumes much time due to several processing steps required to fabricate the cantilevers and subsequently measure the resulting deflections. A less-time consuming approach is to use a finite element model to predict the tip deflection due to the residual stresses across the film thickness. To do this, stress evolution is studied and local stresses are computed for finite layers of poly-SiGe films. The structural layer is then considered as a superposition of finite layers in thickness with each layer sustaining its local stress. It is therefore shown that strain gradient can be estimated fairly accurately from the local stresses in thin films using the finite element model.

2 METHODOLOGY

2.1 Experimental technique

Recipes A and B of poly-SiGe films (Table 1) were used for stress evolutionary study. These recipes were selected by the grey-Taguchi optimization technique [2]. The films were deposited on SiO_2/Si(100) substrate using an Applied Materials Centura LPCVD system. For each recipe, films of different thicknesses were deposited by varying the deposition time between 5 and 565 s. The thickness and residual stress were characterized by FEI Nova 200 Scanning Electron Microscopy (SEM) and FSM 128L stress measurement tool, respectively.

Table 1: Deposition conditions used for evolutionary study

Recipe	T_{dep} (^{o}C)	CP (Torr)	$^{1}B_2H_6$ (sccm)	H_2 (sccm)	HH (mil)
A	415	60	18	500	470
B	415	65	11	500	500

HH = header-shower head spacing ; ^{1}1 % in Hydrogen. The silane and germane (10 % in Hydrogen) flow rates are 8 and 180 sccm, respectively for both recipes.

To determine the strain gradients, ~100 nm thick films were deposited on SiO_2/Si(100) substrate using both recipes. Then, arrays of nanocantilevers were fabricated by surface micromachining following the procedure depicted in Fig. 1 (details in Ref.3). A patterned SiO_2 layer was used as the sacrificial layer below the poly-SiGe layer. The oxide

layer was then removed by using vapour HF to create the freestanding nanostructures. The actual length L and the tip deflection δ of a few nanocantilevers were measured from SEM images and confirmed by AFM images [3]. The strain gradient Γ was calculated from Eq. (1).

$$\Gamma = 2\delta / L^2 \qquad (1)$$

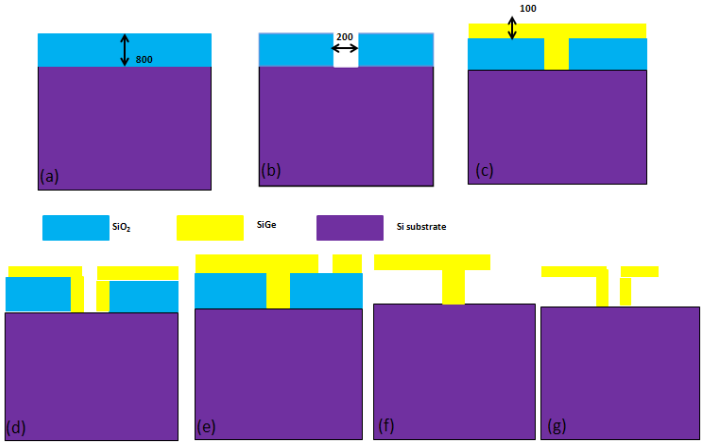

Fig. 1: Fabrication sequence for the nanocantilevers: (a) 800 nm thick SiO_2 layer deposited by LPCVD (b) lithographic definition of the anchor (c) LPCVD deposition of ~100 nm thick poly-SiGe film (d, e) lithographic definition of the cantilever (f, g) sacrificial SiO_2 is removed in hydrofluoric acid. (NB: all dimensions in nm).

2.2 Finite Element Modeling (FEM) technique

Finite element models are constructed and implemented in COMSOL Multiphysics platform [4]. The ~100 nm thick nanocantilevers were modelled as superposition of smaller layers, with each later sustaining its corresponding stress (Fig. 2). The layers form a 'union' and were meshed using the 'physics-controlled mesh' sequence. The material properties of the structure were specified based on the assumption of a linear isotropic condition with elastic deformation. In this case, single values for elastic modulus E (130 GPa [5]), Poisson's ratio ν (0.22 [6]), and coefficient of thermal expansion α, etc. were supplied. Only the local stress was imposed on each layer since the cantilever deflection was mainly due to the intrinsic stress (see section 3). The tip deflection was obtained from the FEM results and the strain gradients were calculated therefrom. The strain gradients so obtained were compared with those of the experiments.

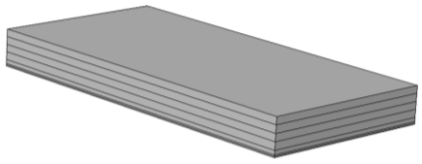

Fig. 2: A 3-D model of the nanocantilever showing superimposed layers

3 RESULTS AND DISCUSSION

3.1 Stress evolution

The intrinsic stresses in films A and B evolve from an initial highly compressive stress regime to a less compressive stress state and stabilize thereafter (Fig. 3a). This behaviour slightly deviates from those of materials (such as Ag and Cu) which exhibit Type I behaviour [7]. Because poly-SiGe has low adatom mobility and low surface and grain boundary diffusivities at low temperature, the tendency for adatom to move into the grain boundary is insignificant [5]. This might be responsible for the constant intrinsic stress observed as film thickens [8]. In addition, no significant stress change is expected when grains grow columnarly as compared with lateral growth [9].

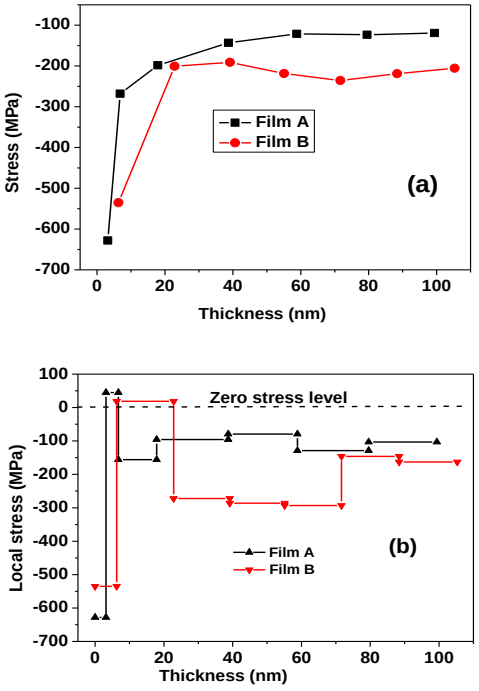

Fig. 3: (a) Evolution of intrinsic stress for recipes A and B (b) calculated local stresses based on Eq. (2).

For the two films, the phenomena leading to the initial highly compressive stress state have been extensively discussed in the literature [10]. With island growth and

coalescence, the grain boundary grows and an average local tensile stress is generated within a very small interval of time. The island precoalescence compressive stress state can also be attributed to capillarity effect of the island surfaces, atomic peening effect, island shape transition and surface stress effect [11]. It should be noted that, unlike those materials that typically exhibit type I and type II behaviour, the tensile stresses generated during coalescence process for poly-SiGe films are insufficient to bring the average stress to a tensile state.

3.2 The local stresses

Local stress refers to the instantaneous stress present in each discrete layer of the film assuming the film to be a superposition of layers with each layer sustaining its corresponding intrinsic stress [9]. The change in the local stress across the film thickness leads to the strain gradient which causes a released structure to deflect upward or downward. The local stress $\sigma_{h_i - h_{i-1}}$ due to an added layer $h_i - h_{i-1}$ can be calculated from Eq. (2).

$$\sigma_{h_i - h_{i-1}} = \frac{\sigma_i}{h_i - h_{i-1}} h_i - \frac{\sigma_{i-1}}{h_i - h_{i-1}} h_{i-1} \qquad (2)$$

where σ_{i-1} and σ_i are the local stresses associated with thickness h_{i-1} and h_i, respectively. Equation (2) implies that the consistency of stress-thickness of discrete layers and that of the equivalent stack must be satisfied. According to Chason et al. [9], the consistency equation for N number of local layers is given by Eq. (3).

$$\sigma h_f = (h_i - h_{i-1}) \sum_{i=1}^{N} \sigma_{h_i - h_{i-1}} \qquad (3)$$

The local stresses are generally less compressive for the film A than for the film B except for the thin slightly tensile layers (Fig. 3b). These local stresses are due to the curvature changes as more film is deposited. It is also observed that the top layer is more compressive for the film B than for the film A thereby induces higher negative strain gradient. Similarly, for a film thickness of ~100 nm, most layers are under compressive stresses with lower magnitude for the film B.

3.3 Experimental and theoretical strain gradients

The nanocantilevers fabricated from films A and B (Fig. 4a and b, respectively) are completely released from the underlying oxide layer as evident from Fig. 4(c). The lengths of the cantilevers vary between ~0.8 µm and ~5 µm while the spacing in-between two neighboring cantilevers is ~200 nm. The tip deflections were measured from SEM images while the strain gradients were calculated from Eq. (1). For the theoretical strain gradient, seven discrete layers were superimposed with each layer sustaining its corresponding intrinsic stress (Fig. 2). The local thickness and the corresponding local stresses are indicated in Fig. 3(b). Due to the variation in the local stresses across the stack, the structural layers deflectes downwardly (Fig. 5). By using the calculated local stresses depicted (Fig. 3b), the results of the FEM (deflections and strain gradients) are plotted together with those of the experiments (Fig. 6 & Fig. 7).

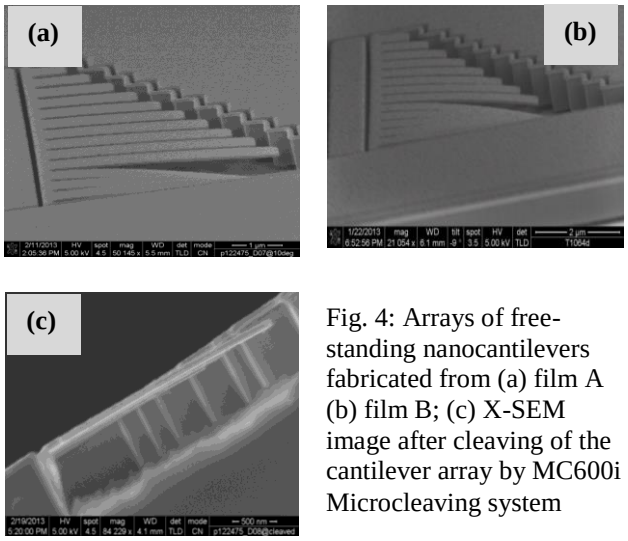

Fig. 4: Arrays of free-standing nanocantilevers fabricated from (a) film A (b) film B; (c) X-SEM image after cleaving of the cantilever array by MC600i Microcleaving system

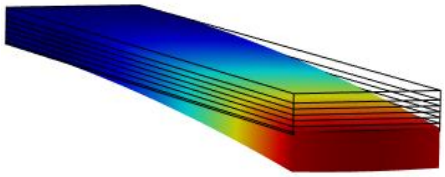

Fig. 5: Cantilever deflection under the influence of local stresses. The color map corresponds to the total displacement from 0 (blue) to 228 nm (red)

For the film A, the experimental average strain gradient is -0.02±0.004 /µm while FEM gives -0.019±0.002 /µm. The former translates to a downward deflection of 10 nm for 1 µm long, 100 nm thick nanocantilevers. Similarly, the experimental average strain gradient for the film B is -0.083±0.009/µm while the FEM gives -0.078±0.007 /µm. These results imply that the strain gradient in the film A is about 4 times lower than that of the film B. The large difference in the strain gradients is due to the corresponding difference in the stress gradients across the film thickness (Fig. 3b). For the film A, the local stresses are more uniform compared to those of film B. In addition, the local stresses are far less compressive thereby reduce the film curvatures. This shows a trend between the stress gradients and the strain gradients across the films. With the stress gradient, it is possible to compare, albeit relatively, the anticipated strain gradients in different released structures.

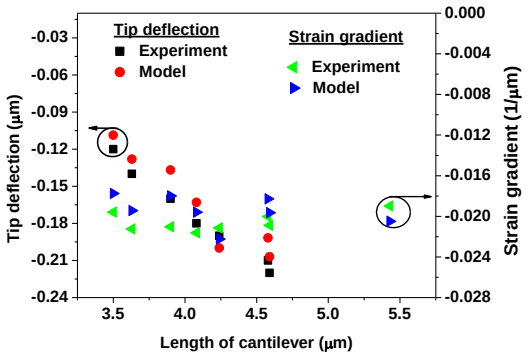

Fig. 6: Tip deflections and strain gradients for film A obtained from the experiment and FEM.

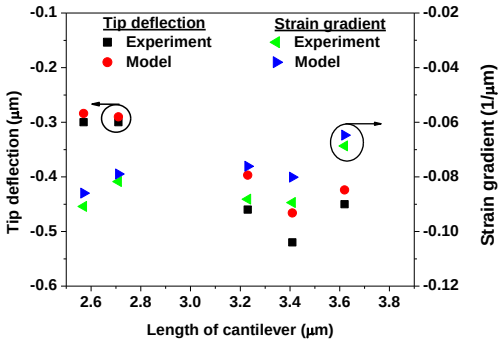

Fig. 7: Tip deflections and strain gradients for film B obtained from the experiment and FEM

The FEM results are very similar to those of the experiments which indicate that the calculated local stresses are close to their actual values. To further confirm that the stress gradient is responsible for the observed strain gradient, a FEM of 100 nm thick layer is subjected to the average residual stress of the stack (-155 MPa). The observed tip deflection (Fig. 8) is very insignificant compared to that of the superimposed layers (Fig. 5). This presupposes that the local stress gradient is more relevant in describing strain gradient than the average stress of the stack.

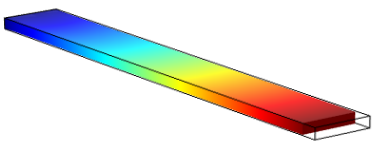

Fig. 8: Deflection of a single-layer cantilever under the influence of average residual stress. The color map corresponds to the total displacement from 0 (blue) to 0.4 nm (red)

4 CONCLUSIONS

A comparative study of experimental and finite element modeling approaches to strain gradient measurement for poly-SiGe nanocantilevers is reported. A careful estimation of strain gradients from the two approaches produces similar values for the films A and B considered. These values are indications of the differences in the local stresses of the two films as measured through the stress evolution study.

References

1. Sedky S. Post-processing techniques for integrated MEMS. London : Aztech House, 2006.
2. Asafa T. B., Bryce G., Severi S., Said S.A.M., Witvrouw. A., Multi-response optimization of ultrathin poly-SiGe films characteristics for nano-electromechanical systems (NEMS) using the grey-Taguchi technique, Microelec. Eng. 2013;11: 229.
3. Asafa, T. B. Development of Ultrathin Poly-SiGe films as a structural layer for applications in nanoelectromechanical systems. PhD Thesis, King Fahd University of Petroleum and Minerals, Dhahran, 2013.
4. COMSOL Multiphysics, Ver. 4.3, Stockholm, Sweden: COMSOL AB, 2010.
5. Asafa T. B., Witvrouw A., Schneider D., Moussa A., Tabet N., Said S.A.M. Thickness effect on the structural and electrical properties of poly-SiGe films. Materials Research Bulletin 2014; 49: 102-107.
6. Hopcroft M.A., Nix W.D., Kenny T. W. What is the Young's Modulus of Silicon? Journal of Microelectromechanical Syst. 2010;19(2): 229-238
7. Freund L.B., Suresh S. Thin Film Materials: Stress, Defects Formation and Surface Evolution. Cambridge : Cambridge University Press, 2003.
8. Sheldon B.W., Rajamani A., Bhandari A., Chason E., Hong S.K., Beresford R. Competition between tensile and compressive stress mechanisms during Volmer–Weber growth of aluminum nitride films. J. Appl. Phys. 2005; 98 (4): 043509.
9. Chason E., Shin J.W., Hearne S.J., Freund L.B. Kinetic model for dependence of thin film stress on growth rate,temperature, and microstructure. J. Appl. Phys. 2012;111: 083520.
10. Hoffman R.W. Stresses in thin films: the relevance of grain boundaries and impurities. Thin Solid Films 1976;34: 185.
11. Nix W.D., Clement M.D. Crystallite coalescence: A mechanism for intrinsic tensile stresses in thin films. J. Mater. Res. 1999;14(8):3467-3473.